ISBN: 978-3-95450-234-9 ISSN: 2673-5504 doi:10.18429/JACoW-SRF2023-TUPTB002

MODELLING TRAPPED FLUX IN NIOBIUM

F. Kramer*, S. Keckert, O. Kugeler, J. Knobloch[1], Helmholtz-Zentrum Berlin, Berlin, Germany
T. Kubo[2], High Energy Accelerator Research Organization (KEK), Tsukuba, Japan
[1]also at Universität Siegen, Siegen, Germany
[2]also at The Graduate University for Advanced Studies (Sokendai), Hayama, Japan

Abstract

Detailed measurements of magnetic flux dynamics and trapped magnetic flux in niobium samples were conducted with a new experimental setup that permits precise control of the cooldown parameters. With this setup the dependency of trapped flux on the temperature gradient, external magnetic field, and cooldown rate can be mapped out in more detail compared to cavity measurements. We have obtained unexpected results, and an existing model describing trapped flux in dependence of temperature gradient does not agree with the measured data. Therefore, a new model is developed which describes the magnitude of trapped flux in dependence of the temperature gradient across the sample during cooldown. The model describes the amount of trapped flux lines with help of a density distribution function of the pinning forces of pinning centers and the thermal force which can de-pin flux lines from pinning centers. The model shows good agreement with the measured data and correctly predicts trapped flux at different external flux densities.

INTRODUCTION

When superconductors transition to the Meissner state all magnetic flux is expelled in an ideal case. However, in experiments it is observed that some fraction of the external magnetic field gets trapped inside the superconductor in form of quantized magnetic flux lines. For the application of superconducting radio frequency (SRF) cavities this trapped flux increases the losses in the cavity wall. For this reason cavities are operated in shielded cryostat which reduce the earth's magnetic field. It is, however, impossible to completely shield off all magnetic field. For this reason research on how to reduce trapped flux is ongoing.

At this point the mechanism of flux trapping is not yet fully understood which makes it difficult to find treatments which effectively reduce flux trapping. To help understand the mechanism we conducted dedicated flux trapping experiments using samples. The experimental setup and the key findings are presented in these proceedings under TUCXA01. In this work the focus lies on a theoretical model which is developed on the basis of the data gathered during these experiments.

The model describes the magnitude of trapped flux with help of a density distribution function $n(f_p)$ which describes the probability of a flux line to interact with a pinning center with pinning force f_p. Whether a flux line gets trapped depends on the thermal force [1] which acts on the flux line. If it is larger than the pinning force the flux line gets pushed over the pinning center and is expelled. If it is smaller than the pinning force the flux line gets pinned and is trapped inside the superconductor.

In the course of this work the gathered data is first compared to an existing model [2] which does not show good agreement. Then the idea of the new model is introduced which is then refined in a next step. Finally, the refined model is applied to the data, and the resulting prediction of trapped flux is compared with measurements.

APPLYING THE EXISTING MODEL

Figure 1 depicts measurement results of trapped flux versus temperature gradient during cooldown (∇T). To measure this curve an external magnetic flux density of 100 µT is set perpendicular to the samples surface during all cooldowns. The cooldown rate is kept constant as well, and only the temperature gradient is changed for each cooldown. The results shown here are recorded with a large grain sample. This sample consists of only two niobium grains (RRR=300) with a grain boundary running through the middle of the sample. The dimensions are $(100 \times 60 \times 3)\,\mathrm{mm}^3$. A model describing the flux trapping mechanism is developed by T. Kubo in Ref. [2]. This model predicts a dependency of trapped flux on the temperature gradient during cooldown that is proportional to $(\nabla T)^{-1}$. Therefore, a fit according to $a/\nabla T + b$ is performed with the data in Fig. 1. The result is also depicted in Fig. 1 in red.

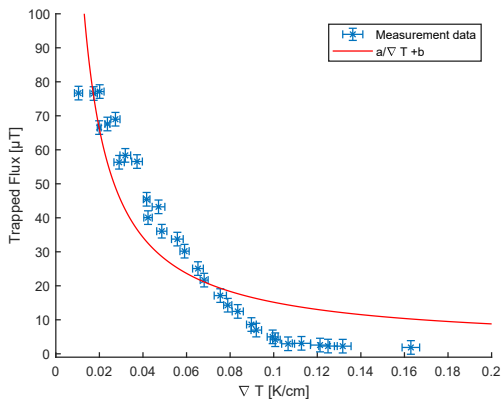

Figure 1: Measurement data of trapped flux versus temperature gradient during cooldown. The data is obtained using a large grain sample consisting only of two grains (sample dimension: $(100 \times 60 \times 3)\,\mathrm{mm}^3$). Additionally, a fit according to the prediction in Ref. [2] is performed and the result is depicted in red.

* f.kramer@helmholtz-berlin.de

ISBN: 978-3-95450-234-9 ISSN: 2673-5504 doi:10.18429/JACoW-SRF2023-TUPTB002

Figure 1 shows no good agreement between measurement and fit. The two main reasons are that the model is developed for a superconductor with sparse pinning centers and a magnetic field applied parallel to the surface. Both requirements are not fulfilled with these measurement points.

THE BASE MODEL

Since the model presented above does not agree with the measurements a new model is developed. Figure 2 shows a schematic depiction of the sample during cooldown at a time t and at a later time $t + \Delta t$. Since the sample is cooled down with a temperature gradient established across the sample, and in an external magnetic field it is in three phases simultaneously. Below x_{c1} the sample is already cold enough that the external flux density B_e is smaller than B_{c1}. Therefore, the sample is in the Meissner state. In the region between x_1 and x_{c2} it holds that $B_{c1} < B_e < B_{c2}$ so that the sample is in the mixed, or Shubnikov state. Above x_{c2} the external flux density is larger than B_{c2} and the sample is normal conducting. During cooldown this region is pushed up the sample.

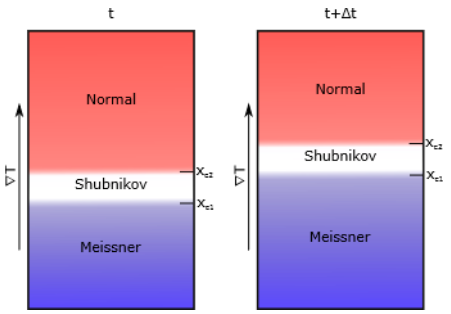

Figure 2: During transition the sample is in three sates simultaneously: Below x_{c1} the sample is cold enough so that the external field is smaller than B_{c1}. Between x_{c1} and x_{c2} the sample is in the mixed state. Above x_{c2} the sample is still normal conducting. During cooldown the transition region moves up the sample.

As x_{c2} moves up the sample new quantized flux lines are formed at the boundary to the mixed state. While they are in the mixed state the thermal force pushes these flux lines towards the colder region and, therefore, x_{c1} and the Meissner state [1]. At this point it is not understood what the flux line dynamics are at the phase transition front to the Meissner state at x_{c1}. For now the following assumption is made: If flux lines are at the position of a pinning center (i.e. they are pinned) when x_{c1} reaches them they are trapped inside the material. If, however, they are not pinned when x_{c1} reaches them, they are expelled.

In Ref. [1] the thermal force is described to be proportional to ∇T so that it can be written as $f_{th} = a\nabla T$ where a is a constant. If this force is larger than the pinning force f_p of a given pinning center the flux line is pushed over it. But since the pinning force of all pinning centers is not known a distribution function $n(f_p)$ is introduced which describes the probability of a flux line to interact with a pinning center with pinning force f_p. It is normalized to fulfill $\int_0^\infty n(f_p)\mathrm{d}f_p = 1$. The density distribution is not known and Fig. 3 shows a hypothetical density distribution. Since different pinning centers might have different underlying pinning mechanisms it is not continuous. The most extreme forces reachable by a given mechanism are labeled f_0 to f_4.

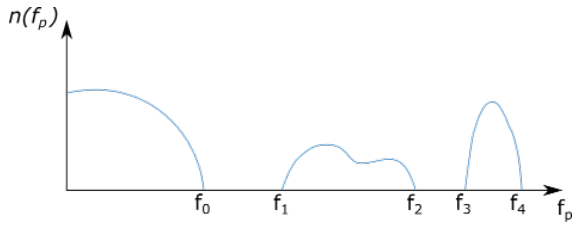

Figure 3: Hypothetical density distribution $n(f_p)$. Due to different pinning mechanism it is not continuous. The most extreme forces reachable by a mechanism are label f_1 to f_4.

With this density distribution the ratio of trapped flux lines (r_{trap}) can be calculated by calculating the ratio of expelled flux lines (r): $r_{trap} = (1 - r)$. To calculate r the density distribution $n(f_p)$ is integrated up to the thermal force f_{th} that is reached in a cooldown

$$r(\nabla T) = \int_{f_p<f_{th}} n(f_p)\mathrm{d}f_p. \tag{1}$$

Equation (1) incorporates that flux lines do not get pinned as long as the pinning force is smaller than the thermal force. In order to make a prediction from this model two assumptions are made:

1. The maximal achievable thermal force is larger than f_0 but smaller than f_1: $f_0 < a|\nabla T|_{max} < f_1$
2. $n(f_p)$ is constant for f_p smaller than f_0: $n(f_p < f_0) = n_0 = const.$

The first assumptions states that the maximal achievable temperature gradient and corresponding thermal force is large enough to push flux lines over weak pinning centers but not strong enough to push flux lines over hard pinning centers. The second assumption is made because $n(f_p)$ is not known and a constant value is a good starting point.

Using these assumptions the ratio of expelled flux lines can be calculated

$$\begin{aligned} r(\nabla T) &= \int_{f_p<f_{th}} n(f_p)\mathrm{d}f_p \\ &= n_0 a|\nabla T|\left[1 - \theta\left(|\nabla T| - \frac{f_0}{a}\right)\right] + n_0 f_0 \theta\left(|\nabla T| - \frac{f_0}{a}\right) \\ &= k|\nabla T|\left[1 - \theta\left(|\nabla T| - \frac{R_w}{k}\right)\right] + R_w\theta\left(|\nabla T| - \frac{R_w}{k}\right), \end{aligned} \tag{2}$$

where θ is the heaviside step function, and k is defined as $k = n_0 a$ with n_0 the constant introduced in assumption 2. R_w is the ratio of weak pinning centres: $R_w = \int_{f_p<f_0} n(f_p)\mathrm{d}f_p = n_0 f_0$. Equation (2) states that the ratio of expelled flux lines increases linearly with ∇T with slope k up to the point where the thermal force equals the maximum force achievable by

ISBN: 978-3-95450-234-9 ISSN: 2673-5504 doi:10.18429/JACoW-SRF2023-TUPTB002

the weak pinning centers f_0. At higher gradients no effect on ∇T is predicted and a constant ratio R_w is expelled. To calculate the trapped flux magnitude (B_{TF}) r_{trap} is multiplied by the external magnetic flux density B_{e}:

$$\begin{aligned} B_{\mathrm{TF}}(\nabla T) &= (1 - r(\nabla T))B_{\mathrm{e}} \\ &= B_{\mathrm{e}} - B_{\mathrm{e}}\left[k|\nabla T|\left[1 - \theta\left(|\nabla T| - \frac{R_w}{k}\right)\right] + \right. \\ &\left. R_w\theta\left(|\nabla T| - \frac{R_w}{k}\right)\right]. \end{aligned} \tag{3}$$

The two fit parameters k and R_w must be determined experimentally. Equivalent to what is already stated with respect to r this model predicts a linear decrease of trapped flux up to the point where the maximal pinning force of weak pinning centers is exceeded. For higher temperature gradients a constant value is predicted. Figure 4 shows the same measurement data as Fig. 1 but now a fit according to Eq. (3) is performed and the result is depicted in red.

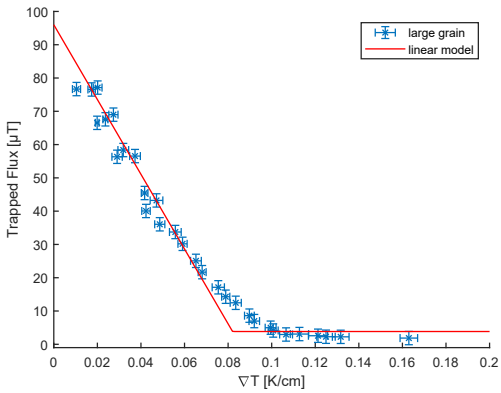

Figure 4: Measurement results gained from the large grain sample and fit results according to Eq.(3).

Figure 4 already agrees better with the measurement data but the curve in the measurement data is not yet represented by the model.

REFINING THE MODEL

In order to refine the model the second assumption that $n(f_{\mathrm{p}})$ is constant below f_0 is dismissed. Instead data gathered at different external magnetic flux densities is investigated and the observed features are translated to a distribution function. Figure 5 shows data of the same large grain sample that is introduced above. For these measurements the temperature gradient and cooldown rate are kept constant within one measurement series and the external magnetic flux density magnitude is altered between 0 µT and 190 µT. The orientation is always kept constant, perpendicular to the sample surface. After sufficient data points are recorded at one temperature gradient a different temperature gradient is set and a new series is recorded. The cooldown rate is always kept constant. In Fig. 5 different series are depicted and color coded.

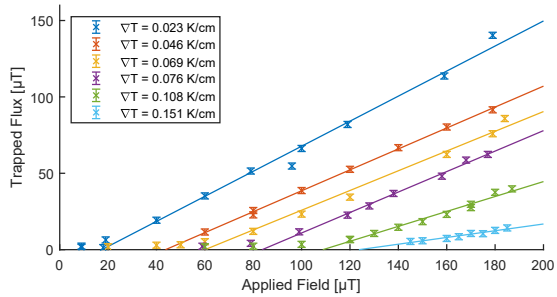

Figure 5: Trapped flux magnitude versus external magnetic flux density. Measurement series at different temperature gradients are depicted and color coded. Measurement points of the same series are fitted with linear regression. The fit results are displayed in the same color.

It is evident that flux only starts to get trapped if the external flux density exceeds a threshold field B^*. Once $B_{\mathrm{e}} > B^*$ trapped flux seems to be increasing linearly. Therefore, a linear regression is performed for each measurement series. In this regression only data point above B^* are included. In Fig.5 the results are depicted in the same color as the measurement points.

The fit parameters of the performed fits can now be plotted versus the temperature gradient of the corresponding measurement series. But since the temperature gradient is not perfectly constant during all cooldown of a series the fit parameters are plotted versus the mean temperature gradient of the measurement points that are used for the fit.

Figure 6 shows the slope of the fits in Fig. 5 versus temperature gradient. For better readability not all measured series are depicted in Fig. 5 but Fig. 6 depicts the slope of all available series which is why there are more data point in Figs. 6, 7, and 8 than there are fits in Fig. 5.

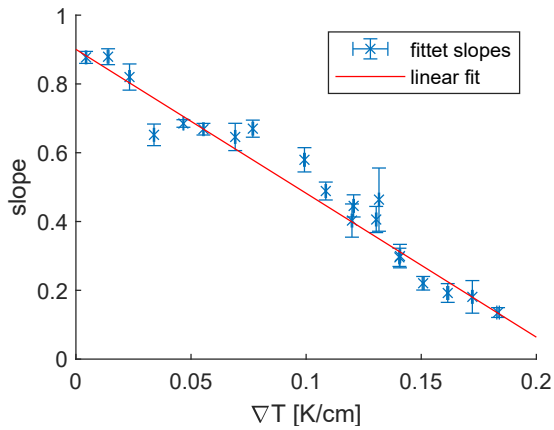

Figure 6: Slope of linear fits in Fig. 5 versus mean temperature gradient of data points used for the fit. Additionally, a fit according to Eq. (4) is depicted. In Fig. 5 not all measured series are depicted for better readability which is why this plot shows more slopes than there are fits in Fig. 5.

ISBN: 978-3-95450-234-9 ISSN: 2673-5504 doi:10.18429/JACoW-SRF2023-TUPTB002

At this point an assumption is made that the slope η of the fits decreases linearly with temperature gradient. It is, therefore, parameterized as

$$\eta(|\nabla T|) = \eta_0 \left(1 - \frac{|\nabla T|}{g_c}\right). \quad (4)$$

The parameterization is chosen like this, so the physical interpretation of the parameters becomes clearer: The slope or "trapping efficiency" η equals a trapping efficiency η_0 at $|\nabla T| = 0\,\frac{\mathrm{K}}{\mathrm{cm}}$, and decreases linearly with $|\nabla T|$ up to a critical temperature gradient g_c. At this gradient the trapping efficiency vanishes.

Next, the x-axis crossing, or threshold field (B^*) is plotted versus temperature gradient. This is depicted in Fig. 7.

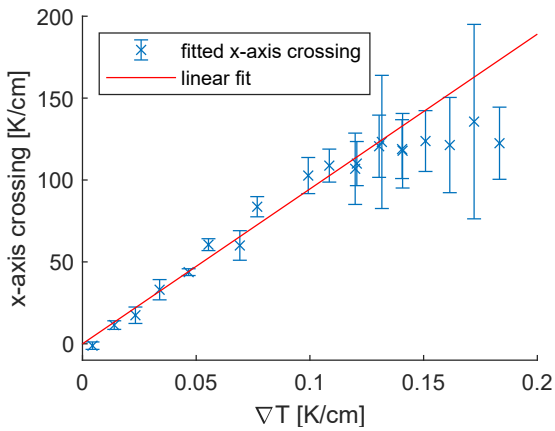

Figure 7: x-axis crossing, or threshold field (B^*), of linear fits in Fig. 5 versus mean temperature gradient of data points used for the fit. In Fig. 5 not all measured series are depicted for better readability which is why this plot shows more data points than there are fits in Fig. 5.

Here, again, an assumption is made that the threshold field increases linearly with increasing temperature gradient. Above a temperature gradient of $\nabla T \approx 0.13\,\frac{\mathrm{K}}{\mathrm{cm}}$ no increase of the threshold field is evident but at the same time the error bars increase strongly. This is caused by the limitations of the setup because at high gradients high external magnetic flux densities are required to trap any flux at all. Since the setup is limited at 190 µT the recorded data points above B^* are close together and also close to zero which makes measurement errors more significant. The series with the highest temperature gradient in Fig. 5 illustrates this problem. This is why a linear increase is assumed and B^* is parameterized as

$$B^*(|\nabla T|) = b\frac{|\nabla T|}{g_c}, \quad (5)$$

where b is the sensitivity of the threshold field on ∇T. Equation (5) is fitted to the data in Fig. 7 and the fit results are depicted in red.

To summarize, three assumptions are made:

1. The dependence of trapped flux on applied field magnitude is linear once flux starts to get trapped above B^* (see Fig. 5).
2. The slope of the linear fits in 1. decreases linearly with increasing temperature gradient (see Fig. 6).
3. The x-axis crossing, or B^*, increases linearly with increasing temperature gradient (see Fig. 7).

Using these three assumptions it follows that the y-axis crossings of the linear fit in Fig. 5 have a component that is quadratic in ∇T. To verify this the y-axis crossings of the fits are plotted versus ∇T and the expected value from the fits according to Eqs. (4) and (5) is also depicted.

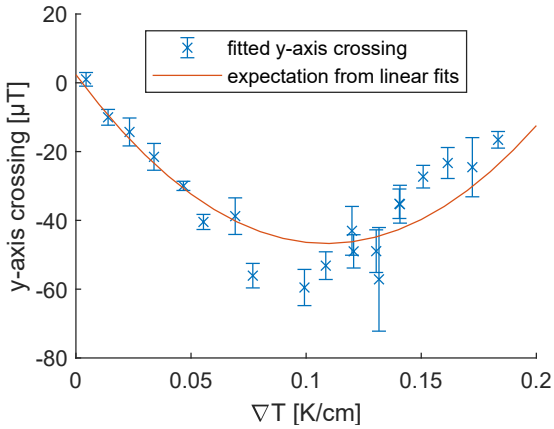

Figure 8: y-axis crossing of linear fits in Fig. 5 versus mean temperature gradient of data points used for the fit. A quadratic dependency on temperature gradient is clearly visible. The prediction from Eqs. (4) and (5) is plotted in red. In Fig. 5 not all measured series are depicted for better readability which is why this plot shows more data points than there are fits in Fig. 5.

In Fig. 8 a quadratic dependency is clearly visible which supports the assumptions that are made.

Using these assumptions and the parameterization for η, and B^* the trapped flux magnitude can be expressed as

$$\begin{aligned} B_{\mathrm{TF}}(B_e, \nabla T) &= \eta(\nabla T)(B_e - B^*(\nabla T)) \\ &= \eta_0 B_e - \eta_0 (B_e + b)\frac{|\nabla T|}{g_c} + \eta_0 b \left(\frac{|\nabla T|}{g_c}\right)^2. \end{aligned} \quad (6)$$

Equation (6) predicts that a fraction η_0 of the applied field is trapped at $\nabla T = 0\,\frac{\mathrm{K}}{\mathrm{cm}}$. With increasing temperature gradient, again, a linear decrease is predicted but now with a quadratic correction term. This equation is, however, only valid as long as $B_e > B^*$. To extend the range at which the model is valid a density distribution function $n(f_p)$ is chosen such that in the range $B_e > B^*$ the model predicts trapped flux according to Eq. (6). It can easily be shown that the following density distribution fulfills this goal

$$n(f_p) = -2\eta_0 \frac{b}{B_e g_c^2 a^2} f_p + \frac{\eta_0}{g_c a}\left(1 + \frac{b}{B_e}\right). \quad (7)$$

ISBN: 978-3-95450-234-9 ISSN: 2673-5504 doi:10.18429/JACoW-SRF2023-TUPTB002

This distribution function is not constant anymore but decreases linearly with f_p. It also includes the external magnetic flux flux density B_e so the effect that the external field has on flux trapping dynamics is also included in this distribution function. With this distribution function the derivation of r and B_{TF} can be done analogous to the derivation shown in the section above. This yields the following Eq. (8) for the trapped flux magnitude:

$$B_{TF}(B_e, \nabla T) = \eta_0 B_e - \left\{ \left[-\eta_0 b \left(\frac{|\nabla T|}{g_c} \right)^2 + \eta_0 (B_e + b) \frac{|\nabla T|}{g_c} \right] \times [1 - \theta(|\nabla T| - \kappa)] + \left[-\frac{\eta_0 b}{g_c^2} \kappa^2 + \frac{\eta_0}{g_c} (B_e + b) \kappa \right] [\theta(|\nabla T| - \kappa)] \right\}, \quad (8)$$

where $\kappa = \frac{f_0}{a}$ is defined which describes the temperature gradient at which the thermal force equals the maximal pinning force of weak pinning centers f_0. For temperature gradient larger than κ the expected trapped flux magnitude stays constant.

Equation (8) can now be fitted to measurement data. Figure 9 shows the same measurement data as before together with a fit according to Eq. (8) as well as the previous fit result obtained from Eq. (3) for comparison.

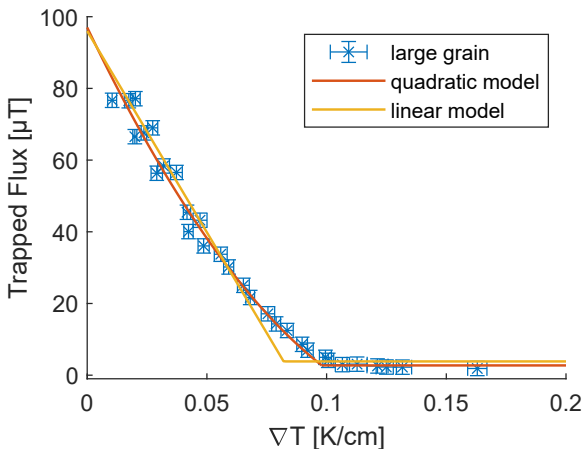

Figure 9: Measurement results obtained with the large grain sample and fit results according to Eq. (8) (red) and the previous model (yellow) for comparison. The refined model shows good agreement with the measurement data.

With the obtained fit parameters Eq. (8) can now also be used to predicts trapped flux when different external magnetic flux densities are applied during cooldown. This is done in Fig. 10 where measurement data of the large grain sample is compared with predictions from the refined model. It must, however, be noted that in order to make predictions the parameter κ must be scaled according to $\kappa(B_e) = \kappa(B_e = 100\,\mu T)\frac{B_e}{100\,\mu T}$. Since the origin of the threshold field is not understood yet no physical interpretation of this scaling can be given at this point.

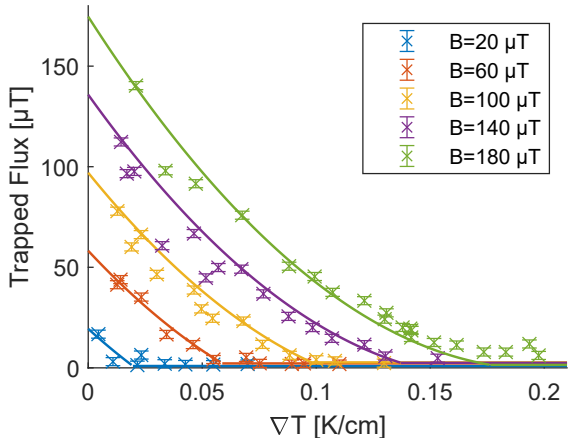

Figure 10: Trapped flux versus temperature gradient data obtained with the large grain sample. Different measurement series at different external magnetic flux densities are depicted and color coded. The solid lines represent the predictions from Eq. (8) with fit parameters obtained from Fig. 9.

The predictions show good agreement with the measurement data. The slower decrease at high fields and high gradients is also correctly predicted.

SUMMARY AND OUTLOOK

With help of data obtained with dedicated flux trapping measurements a new phenomenological model is developed which describes trapped magnetic flux density magnitude in superconducting niobium in dependence of the temperature gradient during cooldown and the applied external magnetic field. Figure 10 shows that the model correctly predicts trapped flux at different external magnetic flux densities once the fit parameters are obtained.

The model also revealed where there still open questions. Most importantly what are the flux line dynamics at the phase transition to the Meissner state and what is the origin of the threshold field.

Further measurements are planned in order to gain better insight in these open questions.

REFERENCES

[1] R. P. Huebener, "Superconductors in a temperature gradient," *Supercond. Sci. Technol.*, vol. 8, no. 4, pp. 189–198, 1995. doi:10.1088/0953-2048/8/4/001

[2] T. Kubo, "Flux trapping in superconducting accelerating cavities during cooling down with a spatial temperature gradient," *Prog. Theor. Exp. Phys.*, vol. 2016, no. 5, 053G01, 2016. doi:10.1093/ptep/ptw049